$$\begin{aligned}\beta &= F_{1c}\cos t\cos\omega t + F_{1s}\sin t\cos\omega t \\ &+ F_{2c}\cos t\sin\omega t + F_{2s}\sin t\sin\omega t + \ldots \\ &= A_{1c}\cos(1+\omega)t + A_{1s}\sin(1+\omega)t \\ &+ A_{2c}\cos(1-\omega)t + A_{2s}\sin(1-\omega)t + \ldots\end{aligned} \tag{5}$$

Equating the coefficients of the 4 harmonics we have

$$\begin{aligned}F_{1c} &= A_{1c} + A_{2c}, \quad F_{1s} = A_{1s} + A_{2s} \\ F_{2c} &= A_{1s} - A_{2s}, \quad F_{2s} = A_{2c} - A_{1c}\end{aligned} \tag{6}$$

In order to obtain the tilting response in the form of Eqs. (2) and (3) we merely have to determine from the measured flapping response $\beta(t)$ the 4 Fourier coefficients for the harmonics $1+\omega$ and $1-\omega$ and then use Eq. (6). The base frequency for the Fourier analysis of the response $\beta(t)$ must be selected such that both $1+\omega$ and $1-\omega$ are integer multiples of this base frequency.

In an air frame fixed reference system and using again complex notation we have from Eq. (1) the cyclic pitch excitation

$$\left.\begin{aligned}\theta_I &= -i|\theta|\exp(-i\omega t) \text{ forward} \\ \theta_{II} &= |\theta|\exp(-i\omega t) \quad \text{left}\end{aligned}\right\} \text{ control} \tag{7}$$

and from Eqs. (2) and (3) the tilting response

$$\left.\begin{aligned}\beta_I &= (F_{1c} + iF_{2c})\exp(-i\omega t) \text{ forward} \\ \beta_{II} &= (F_{1s} + iF_{2s})\exp(-i\omega t) \text{ left}\end{aligned}\right\} \text{ tilt} \tag{8}$$

For unit cyclic pitch, $|\theta| = 1$, the response amplitudes are

$$\left.\begin{aligned}|\beta_I| &= (F_{1c}^2 + F_{2c}^2)^{1/2} \\ |\beta_{II}| &= (F_{1s}^2 + F_{2s}^2)^{1/2}\end{aligned}\right\} \tag{9}$$

The phase differences between response and input are

$$\left.\begin{aligned}\psi_I &= \text{ang}\beta_I - \text{ang}\theta_I = \text{ang}(F_{1c} + iF_{2c}) + \pi/2 \\ \psi_{II} &= \text{ang}\beta_{II} - \text{ang}\theta_{II} = \text{ang}(F_{1s} + iF_{2s})\end{aligned}\right\} \tag{10}$$

Examples of the measured and computed tilting response amplitudes according to Eq. (9) are shown in Figs. 2 and 3.

The preceding method of separating the cyclic control response from the trim response does not work for $\omega = 0$ so that for steady control inputs the trim response must be measured separately and subtracted from the total response. Data processing according to the preceding equations was performed from the magnetic tape records on a PDP-12 analog-digital converter and computer.

Figs. 2 and 3 show for zero rotor shaft angle, 5° collective pitch setting and advance ratios 0 and 0.2, respectively a comparison of analytical (solid lines) and test (dash lines) amplitudes per unit cyclic pitch input. For $\omega = 0.2$, corresponding to the blade natural frequency, the two curves intersect indicating the absence of a wake effect. At other frequencies large systematic deviations in test response from the analytical response occur, following the trend of the qualitative model explained before. Reference 6 includes more test conditions and also phase angle plots from Eq. (8). The data processing method given in Ref. 6 is somewhat different from that given here. The results are the same.

Conclusions

Progressing and regressing rotor flapping modes can be easily excited with a very simple two-bladed rotor model with only 3 control bearings. The unsteady wake effects are largest at zero advance ratio and low collective pitch, but they remain significant at higher advance ratios and collective pitch settings. A more detailed study of the phenomenon to cover a wider test envelope, ground effects and direct wake measurements is in progress.

References

[1]Miller, R. H., "Rotor Blade Harmonic Air Loading," *AIAA Journal*, Vol. 2, No. 7, July 1964, p. 1260.

[2]Ormiston, R. A. and Peters, D. C., "Hingeless Rotor Response with Nonuniform Inflow and Elastic Blade Bending," *Journal of Aircraft*, Vol. 9, No. 10, Oct. 1972, pp. 730–736.

[3]Pierce, G. A. and White, W. F., Jr., "Unsteady Rotor Aerodynamics at Low Inflow and its Effects on Flutter," AIAA Paper 72-959, Palo Alto, Calif., 1972.

[4]Kuczinski, W. A., Sharpe, D. L., and Sissingh, G. J., "Hingeless Rotor Experimental Frequency Response and Dynamic Characteristics with Hub Moment Feedback Controls," 28th Annual National Forum of the American Helicopter Society, Preprint 612, May 1972.

[5]Hohenemser, K. H. and Yin, S. K., "Some Applications of the Method of Multiblade Coordinates," *Journal American Helicopter Society*, Vol. 17, No. 3, July 1972, pp. 3–12.

[6]Hohenemser, K. H. and Crews, S. T., "Unsteady Wake Effects on Progressing/Regressing Forced Rotor Flapping Modes," AIAA Paper 72-957, Palo Alto, Calif., 1972.

Conformal Mapping for Potential Flow about Airfoils with Attached Flap

Vernon J. Rossow*
NASA Ames Research Center, Moffett Field, Calif.

Introduction

A SURPRISINGLY large number and wide variety of conformal transformations using complex variables are presented in the literature for changing one shape into another (see Betz,[1] Kober,[2] Nehari[3]). A number of these transformations have been used to map a known two-dimensional flowfield into a desired one. For example, most aerodynamicists are familiar with the method developed by Theodorsen[4] as an extension of the Joukowski and Karman-Trefftz transformations which maps the flow about a circular cylinder into that about a specified airfoil. Recently, the Karman-Trefftz method for one circular cylinder/airfoil has been extended by Williams[5] so that the flow about two nearby circles can be mapped into the flow about two lifting airfoils (or about an airfoil with a detached flap). These exact incompressible potential flow solutions are not only useful in themselves but they also serve as reference or check cases for numerical and approximate methods.

The purpose of this Note is to present a conformal mapping sequence that transforms the potential flow about a circle into that about an airfoil with an attached flap or spoiler. This method is indirect in that the shape of the flap must be iterated upon by varying parameters in the mapping equations until the resulting flap shape approximates the specified one.

Mapping Sequence

The transformation developed for generating the flap on the airfoil is illustrated in Fig. 1 as 10 steps from a circle

Received September 28, 1972.
Index categories: Airplane and Component Aerodynamics; VTOL Aircraft Design.

* Staff Scientist.

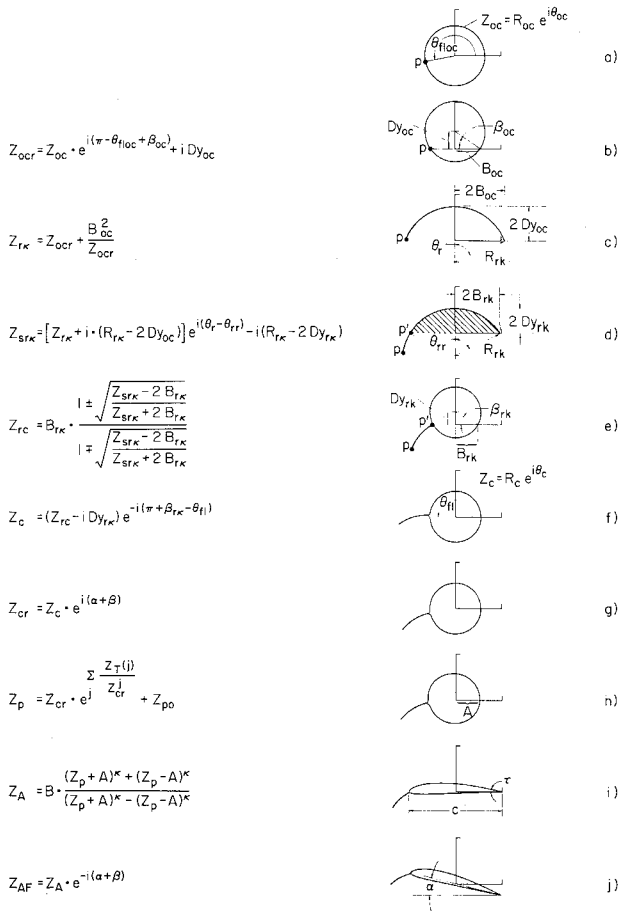

Fig. 1 Steps in mapping sequence illustrated for $\beta_{rk} = +0.5$, $\alpha = 0.3$, $\Theta_{fl} = -3.2$, $L_{fl} = 0.2$.

to the flapped airfoil.† The mapping equations are shown beside each figure. The amounts of rotation and translation given to the circle and arc during the various steps govern the length of the flap, its curvature, and its location on the airfoil. A flap-curvature parameter β_{rk} and a flap-length parameter L_{fl} are used to govern the mapping of the original circle into a circular slit (Z_{rk} plane), to rotate and shift the slit (Z_{srk} plane), and to map the shortened arc into a circle with a flap (Z_c plane). The mapping functions used to obtain this figure must be such that the circular portion is an exact circle of radius R_c (Fig. 1f) so that it can be transformed into an airfoil by Theodorsen's method.[4] Therefore, once the angle that locates the flap in the circle plane (i.e., Θ_{fl} in Fig. 1f) and the parameters β_{rk} and L_{fl} are chosen, the other quantities in the mapping sequence are determined by the following equations:

$$Dy_{rk} = R_c \cdot \sin\beta_{rk};\quad B_{rk} = R_c \cdot \cos\beta_{rk}$$

$$R_{rk} = R_c/\sin\beta_{rk};\quad \theta_{rr} = 2 \cdot \beta_{rk}$$

$$\theta_r = \theta_{rr}(1 + L_{fl});\quad B_{oc} = (R_{rk} \cdot \sin\theta_r)/2$$

$$Dy_{oc} = R_{rk}(1 - \cos\theta_r)/2$$

$$\beta_{oc} = \tan^{-1}(Dy_{oc}/B_{oc}) = \theta_r/2$$

$$R_{oc} = B_{oc}/\cos\beta_{oc}$$

The amount of rotation in the various planes must be

†The Clark Y airfoil[6] was used in all the illustrations because the coefficients $Z_T(j)$ were available from another investigation.

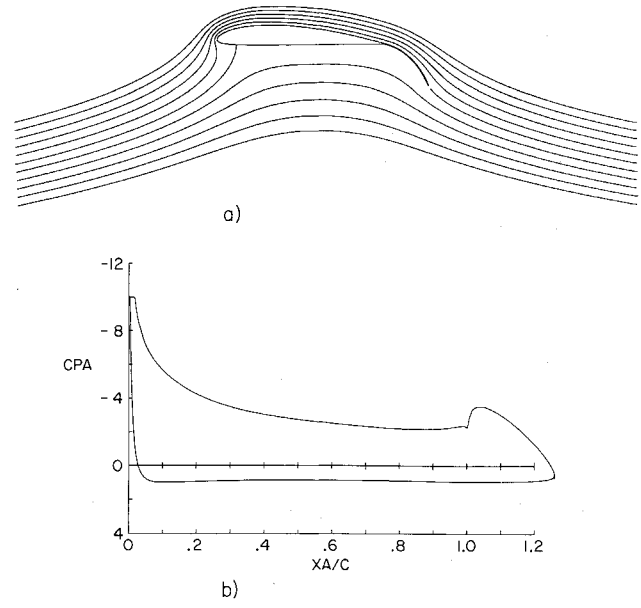

Fig. 2 Flow about airfoil with attached trailing-edge flap; $\alpha = 0.1$, $\beta_{rk} = -0.5$, $\Theta_{fl} = -0.1$, $L_{fl} = 0.33$, $(\Gamma/2\pi U\ c) = -2.53$, $C_L = 5.06$, $C_D = 0$. a) Streamlines, b) pressure distribution.

such that the freestream returns to its original direction in both the circle (or Z_c) and in the final (or Z_{AF}) planes. The various angles are then related by

$$\theta_{floc} = \theta_{fl} - \beta_{rk} + \beta_{oc} + \theta_r - \theta_{rr}$$

where Θ_{floc} locates the tip of the flap in the original circle plane as shown in Fig. 1. The flap-curvature parameter is limited in that it cannot exceed 90°; i.e., $-\pi/2 \le \beta_{rk} \le +\pi/2$. Likewise, the angular segment of the circular arc slit in Fig. 1c cannot exceed 2π, so

$$|\theta_r| \le \pi$$

The flap-length parameter is therefore limited by

$$0 \le L_{fl} \le [(\pi/2|\beta_{rk}|) - 1]$$

The quantities used in the transformation of the flapped circle (Fig. 1f) into the flapped Clark Y airfoil at angle of attack (Fig. 1j) are: the angle of attack of the airfoil from zero lift α; the angle of zero lift from the geometric chord line β; the Theodorsen coefficients $Z_T(j)$, and the shift of the potato curve as listed below:

$$\begin{aligned}
\beta &= -0.05906\\
Z_T(1) &= (-0.07671 + i \cdot 1.18942) \cdot 10^{-3}\\
Z_T(2) &= (+1.22322 - i \cdot 1.25433) \cdot 10^{-3}\\
Z_T(3) &= (-0.04961 + i \cdot 0.07613) \cdot 10^{-3}\\
Z_T(4) &= (+0.01615 - i \cdot 0.05246) \cdot 10^{-4}\\
Z_T(5) &= (+0.6174 + i \cdot 0.1708) \cdot 10^{-6}\\
Z_T(6) &= (-0.5788 + i \cdot 0.6464) \cdot 10^{-7}\\
Z_{po} &= -0.019332 + i \cdot 0.020158
\end{aligned}$$

The parameters A and κ are related to the trailing-edge angle τ, the nose radius R_n, and the chord of the airfoil by

$$\kappa = 2 - \tau/\pi = 1.91487;\quad A = (c - R_n/2)/\kappa = 0.26088$$

It is convenient to relate the various lengths to the chord, c, of the airfoil so that they are dimensionless.

Once the flapped circle has been generated, the flap portion of the figure is carried along without special attention while the circle portion is being mapped into the desired airfoil at angle of attack. During this process, the flap or segment of the arc originally dedicated to the flap

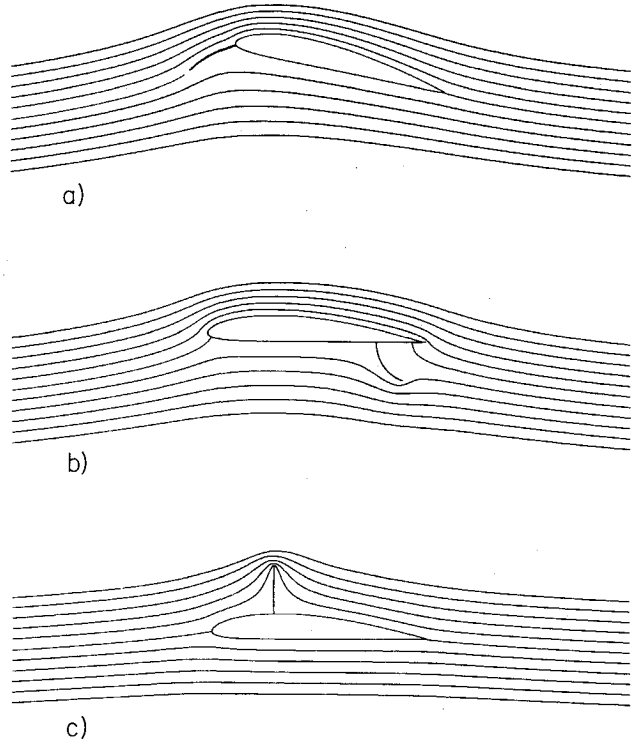

Fig. 3 Streamline pattern about airfoil with three different flaps generated by transformation. a) leading-edge flap: α = 0.3, β_{rk} = +0.5, θ_{fl} = −3.2, L_{fl} = 0.2, $(\Gamma/2\pi cU_\infty)$ = −1.09, C_L = 2.88, C_D = 0; b) split flap: α = 0.1, β_{rk} = +1.0, θ_{fl} = −1.0, L_{fl} = 0.1, $(\Gamma/2\pi cU_\infty)$ = −1.0, C_L = 2.0, C_D = 0; c) spoiler flap: α = 0.1, β_{rk} = −0.4, θ_{fl} = 1.94, L_{fl} = 0.06, $(\Gamma/2\pi cU_\infty)$ = −0.492, C_L = 0.984, C_D = 0.

is carried along as a vanishingly small slit. Its shape is modified from circular in the Z_{rk} and Z_{srk} planes to a nondescript shape in the final airfoil plane. This shape can differ considerably from the original one in curvature and length, making it necessary to iterate on the various flap parameters to arrive at a shape that approximates the desired one.

The only step in the mapping sequence where special attention must be given to the signs or roots of the functions is the one shown in Fig. 1e where the square root is taken. A continuous mapping is obtained if the lower sign on the square root is used when Z_{srk}, the point being transformed, lies within the cross-hatched area between the horizontal or real axis and the arc as shown in Fig. 1d. The upper sign is used when the point is elsewhere in the flow field. This assures the development of both the upper and lower segments of the circle from the circular arc slit. In the calculations, it is convenient to let the original circle be slightly larger than the theoretical value (i.e., increase R_{oc} by 0.0001) to make it possible for the computer to discern whether a point is on the upper or lower portion of the circular arc slit.

The velocity components are found in each of the planes from

$$d\Phi/dZ_{AF} = (d\Phi/dZ_{oc})(dZ_{oc}/dZ_{AF}) = u - iv$$

where

$$\Phi = \phi + i\psi = U_\infty(Z_{oc} + R_{oc}^2/Z_{oc}) - (i\Gamma/2\pi)\ \ln Z_{oc}$$

The streamline pattern, pressures, etc., can then be calculated in closed form for the airfoil with its attached flap after the derivatives dZ_{oc}/dZ_{AF} are found from the mapping functions.

Discussion of Examples

Flow over a Clark Y airfoil with a trailing-edge flap, a leading-edge flap, a split flap, and a spoiler are shown in Figs. 2 and 3 to illustrate the kinds of flaps and flowfields that can be produced by the foregoing technique. The streamlines shown in these cases were found by mapping them from the original circle plane using the flapped-airfoil mapping functions. They could also have been calculated directly in the final airfoil plane using the velocity components and stream function in that plane. The circulation for the airfoil with a split flap shown in Fig. 1b was arbitrarily chosen as a value between that which would yield smooth flow off the trailing edge and off the end of the flap because it was not clear how the Kutta condition should be specified in that case. Also, since the flow about the spoiler shown in Fig. 3c is a potential solution, it does not include the separation of the flow and the unsteady oscillations that usually occur behind the spoiler in a real flowfield.

As indicated previously, the length and amount of curvature of the flap can be varied over wide limits and the flap attachment point can be located anywhere on the surface of the airfoil. The flap can be bent in either direction but the amount of bending cannot be varied along the flap in a specified manner. Also, this transformation forces the flap to intersect the airfoil surface perpendicularly. Although it was not explored, it is felt that an intersection at another angle can probably be obtained by use of an added mapping such as the Schwartz-Christoffel transformation. Also, the flaps presented here are of vanishingly small thickness. A flap with thickness and with a fillet or fairing at its juncture with the airfoil can be obtained by choosing the radius of the original circle larger than the theoretical one by $0.01c$ to $0.1c$, depending on the thickness desired. However, when this is done the circular shape in the flapped-circle plane is no longer an exact circle so that the resulting airfoil differs from the specified one. Finally, an airfoil with two flaps can also be generated by shifting and rotating the circular-arc slit so that the flapped circle is mapped from the center portion of the arc rather than from one end. This technique will produce two flaps on the airfoil, only one of which can be placed arbitrarily because the location of the other one is automatically determined by the location of the other end of the arc.

Concluding Remarks

The conformal mapping sequence presented here and some possible variations that were discussed yield the exact potential flow about an airfoil with an attached flap or spoiler. Adequate versatility of flap shape for a given airfoil can usually be obtained with the indicated functions, although other transformations would expand the variety of possible flap shapes.

References

[1]Betz, A., *Konforme Abbildung*, Springer-Verlag, Berlin, Germany, 1948.

[2]Kober, H., *Dictionary of Conformal Representations*, Dover, New York, 1952.

[3]Nehari, Z., *Conformal Mapping*, McGraw-Hill, New York, 1952.

[4]Theodorsen, T., "Theory of Wing Sections of Arbitrary Shape," TR 411, 1932, NACA.

[5]Williams, B. R., "An Exact Test Case for the Plane Potential Flow About Two Adjacent Lifting Aerofoils," TR 71197, Sept. 1971, Royal Aircraft Establishment, Farnsborough, Hampshire, England. shire, England.

[6]"Aerodynamic Characteristics of Airfoils-IV," TR 244, 1926, NACA.